CHEMISTRY OF MATERIALS

pubs.acs.org/cm Article

Modulating BODIPY-Based Silver Chalcogenide Cluster-Based Metal–Organic Frameworks for Real-Time Decontamination of a Gaseous Sulfur Mustard Simulant

Meng Zhang,[†] Man Cao,[†] Zhi-Bing Sun, Zhen Han, Zhao-Yang Wang, Qian-You Wang,* and Shuang-Quan Zang*

Published on: 22 November, 2023

Corresponding authors:

Qian-You Wang - Henan Key Laboratory of Crystalline Molecular Functional Materials, Green Catalysis Center, and College of Chemistry, Zhengzhou University, Zhengzhou, China

Shuang-Quan Zang - Henan Key Laboratory of Crystalline Molecular Functional Materials, Green Catalysis Center, and College of Chemistry, Zhengzhou University, Zhengzhou, China

29 June 2024 **Samapti Mondal**

Introduction

bis(2-chloroethyl)sulfide

Sulfur mustard or HD

Chemical warfare agent

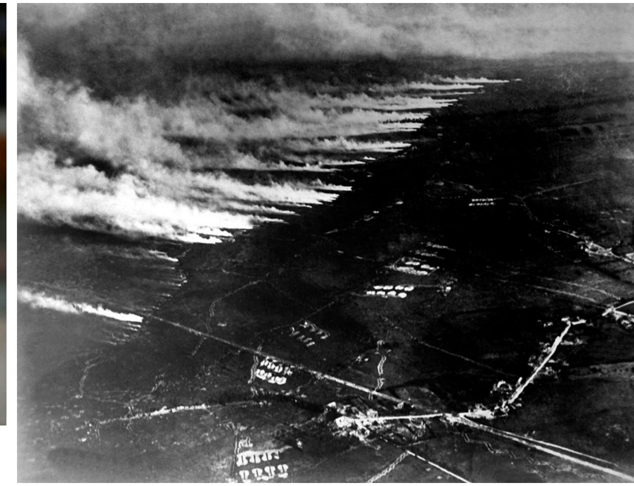

World war- I

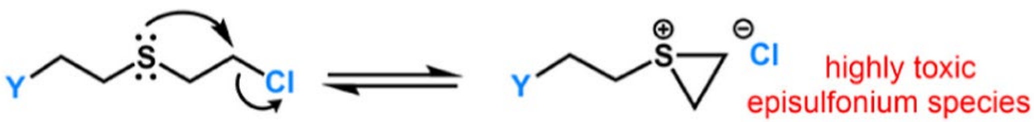

HD (Y=Cl)
CEES (Y=H)

epi-HD (Y=Cl)
epi-CEES (Y=H)

2-chloroethyl ethyl sulfide

CEES (Simulant of HD)

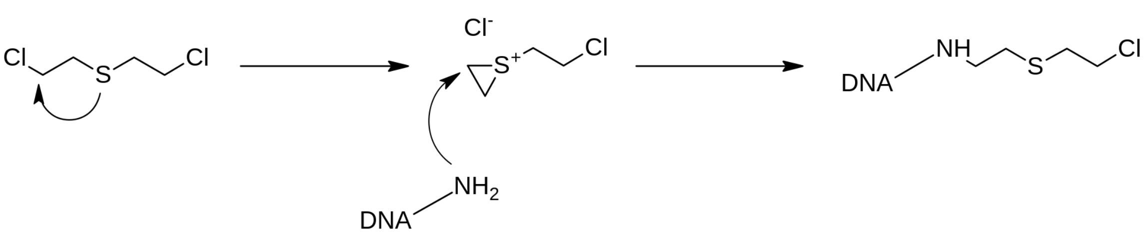

Mustard gas alkylating an amino group via conversion to a episulfonium ion

Introduction

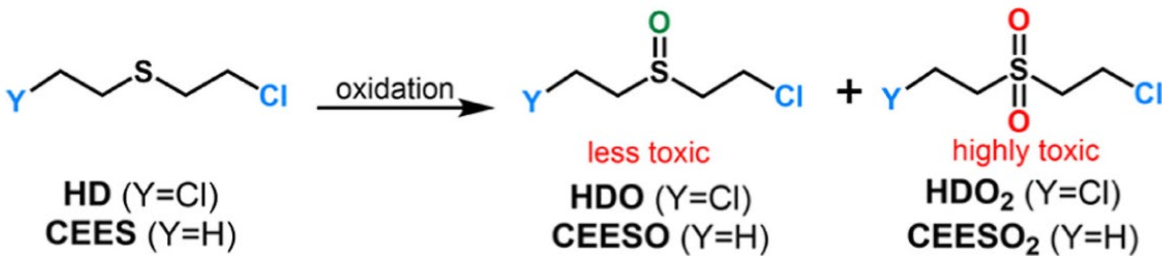

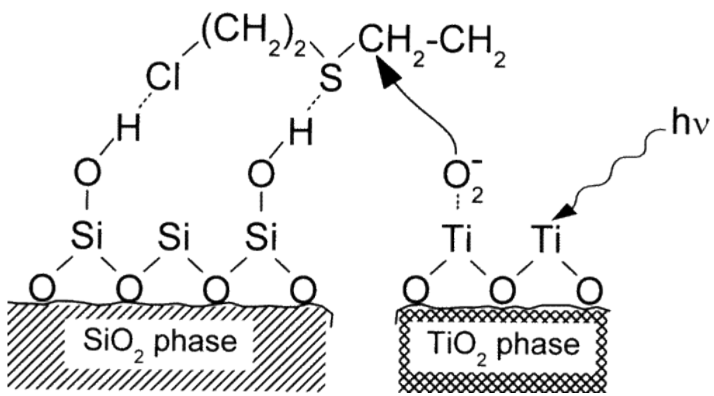

D. A. Panayotov, et al., *J. Phys. Chem. B* **2003**, *107*,10571-10575

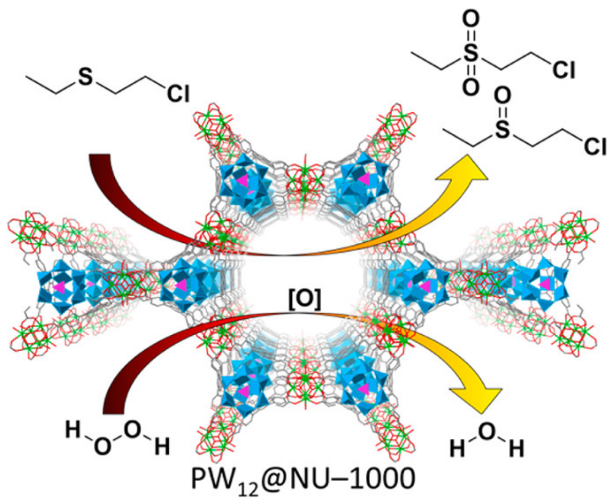

J. T. Buru, et. al., *Chem. Mater.* **2017**, *29*, 5174–5181.

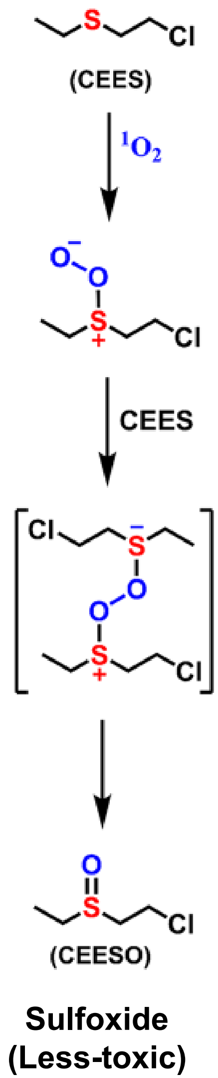

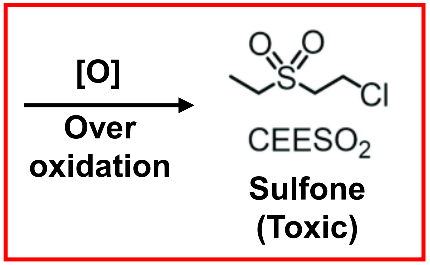

Background

nature > nature materials > letters > article

Letter | Published: 16 March 2015

Destruction of chemical warfare agents using metal–organic frameworks

Joseph E. Mondloch, Michael J. Katz, William C. Isley III, Pritha Ghosh, Peilin Liao, Wojciech Bury, George W. Wagner, Morgan G. Hall, Jared B. DeCoste, Gregory W. Peterson, Randall Q. Snurr, Christopher J. Cramer, Joseph T. Hupp & Omar K. Farha

How to cite: *Angew. Chem. Int. Ed.* **2022**, *61*, e202207130
International Edition: doi.org/10.1002/anie.202207130
German Edition: doi.org/10.1002/ange.202207130

Covalent Organic Frameworks

Aminal-Linked Porphyrinic Covalent Organic Framework for Rapid Photocatalytic Decontamination of Mustard-Gas Simulant

*Qian-You Wang, Jing Liu, Man Cao, Jia-Hua Hu, Rui Pang, Shan Wang, Muhammad Asad, Yong-Li Wei, and Shuang-Quan Zang**

ACS MATERIALS LETTERS
www.acsmaterialsletters.org

Co-assembly of Ag_{29} Nanoclusters with $Ru(bpy)_3^{2+}$ for Two-Photon Up-Conversion and Singlet Oxygen Generation

Jia-Yin Wang, Ya-Ke Li, Xu Jing, Peng Luo, Xi-Yan Dong,* and Shuang-Quan Zang*

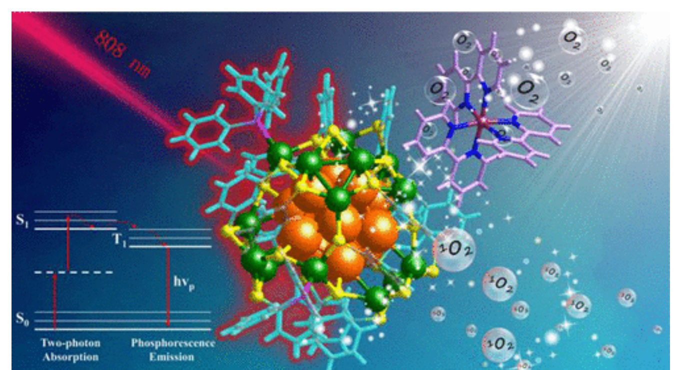

Background

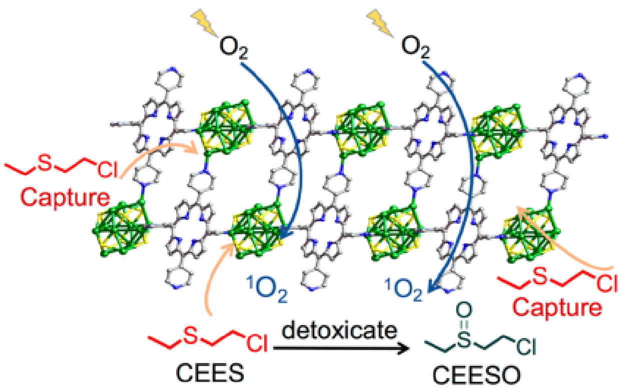

JACS
JOURNAL OF THE AMERICAN CHEMICAL SOCIETY
Communication
Cite This: J. Am. Chem. Soc. 2019, 141, 14505–14509
pubs.acs.org/JACS

Porphyrinic Silver Cluster Assembled Material for Simultaneous Capture and Photocatalysis of Mustard-Gas Simulant

Man Cao,[†] Rui Pang,[‡] Qian-You Wang,[*,†] Zhen Han,[†] Zhao-Yang Wang,[†] Xi-Yan Dong,[†] Shun-Fang Li,[‡] Shuang-Quan Zang,[*,†] and Thomas C. W. Mak[†,§]

JACS
JOURNAL OF THE AMERICAN CHEMICAL SOCIETY
pubs.acs.org/JACS
Article

Post-Synthetically Elaborated BODIPY-Based Porous Organic Polymers (POPs) for the Photochemical Detoxification of a Sulfur Mustard Simulant

Ahmet Atilgan,[#] M. Mustafa Cetin,[#] Jierui Yu, Yassine Beldjoudi, Jian Liu, Charlotte L. Stern, Furkan M. Cetin, Timur Islamoglu, Omar K. Farha, Pravas Deria,* J. Fraser Stoddart,* and Joseph T. Hupp*

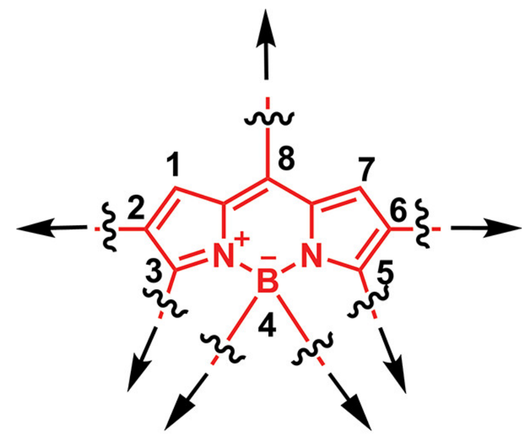

BODIPY Core

Primary requirement of HD aerosol detoxification:

- Efficient capture
- Rapid decontamination
- Need of catalyst suitable in various environmental conditions

Motivation

- Boron-dipyrromethene derivative (BODIPY) possess tunable structure and unique photophysical property – a promising photoactive linker
- Silver clusters with abundant heavy elements at the kernel are promising $^1O_2$ producing catalyst.
- Incorporation of heavy halogen functionalized BODIPY into cluster-MOFs can precisely increase $^1O_2$ generation efficiency.

Why this paper?

- They successfully obtained, for the first time, a series of atomically precise cluster-assembled materials for efficient detoxification of gaseous HD simulant using a family of functional BODIPY ligands from monodentate to multidentate
- Among those, Ag_{12}-BDP-I acts as a robust and porous photocatalyst for efficient real-time adsorption and detoxification of gaseous CEES under various environmental conditions.

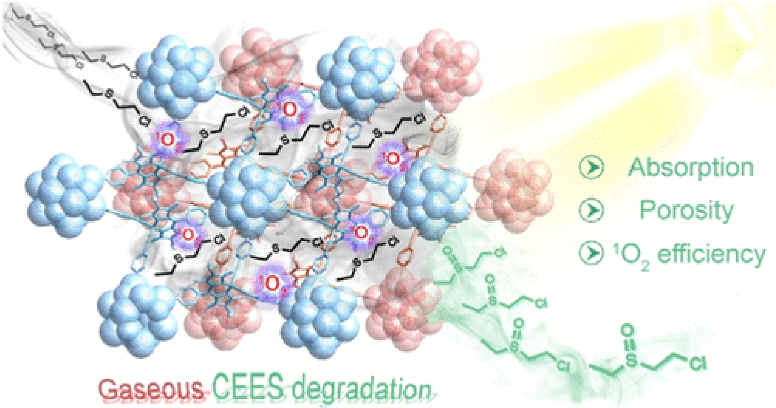

Results and discussion

AgS^{t}Bu + CF_3COOAg (1 : 1) in EtOH/ACN ✚ BDP linker ⟶ Slow evaporation

$[Ag_{12}(S^tBu)_6(CF_3COO)_6(BDP)_6]$

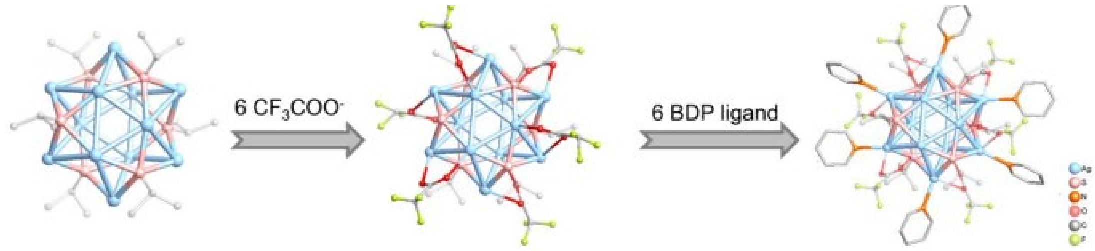

Figure S3. The structure and coordination mode of BDP ligand modified Ag_{12} cluster.

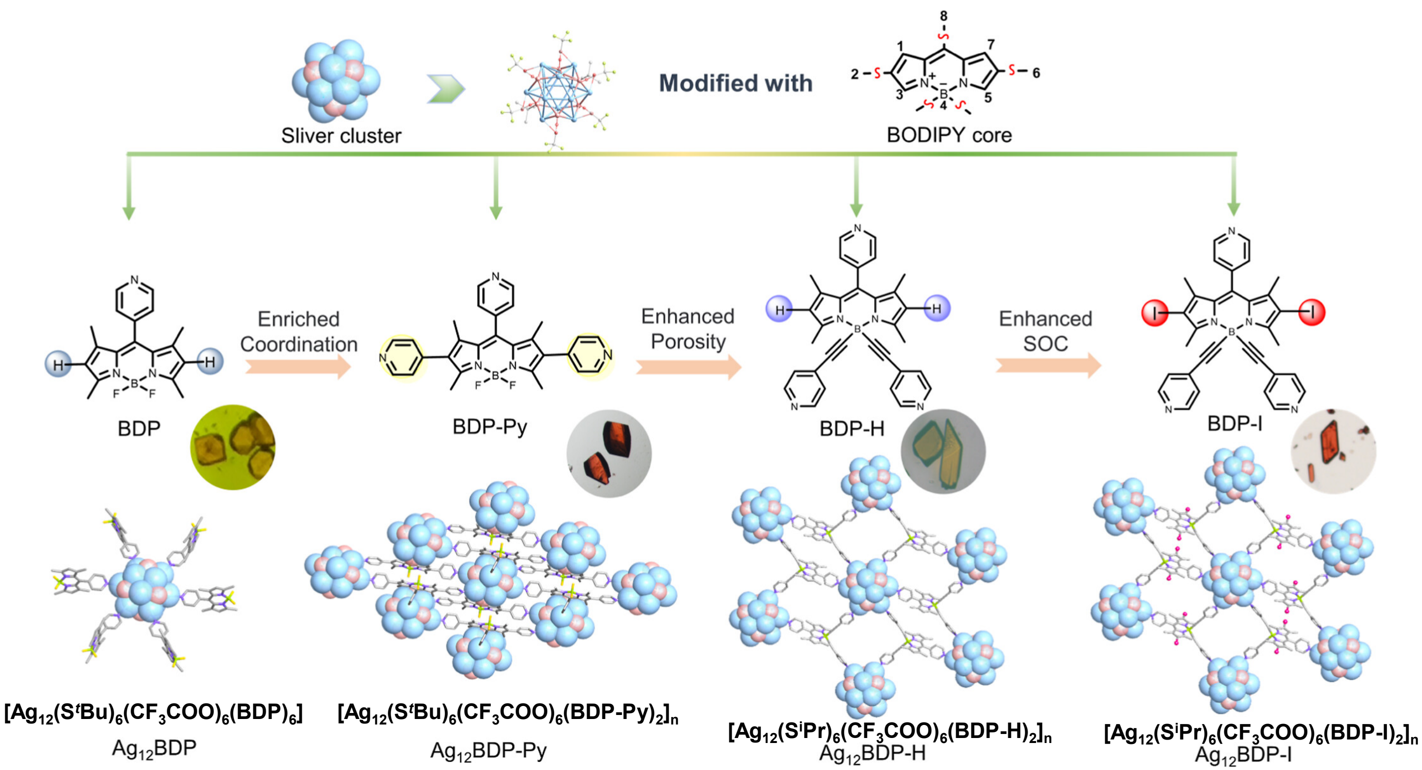

Figure 2. Simplified models of Ag12 cores and BODIPY. Structures and photographs of **Ag_{12}–BDP**, **Ag_{12}–BDP-Py**, **Ag_{12}–BDP-H**, and **Ag_{12}–BDP-I** and the corresponding organic linkers of BDP, BDP-Py, BDP-H, and BDP-I.

Results and discussion

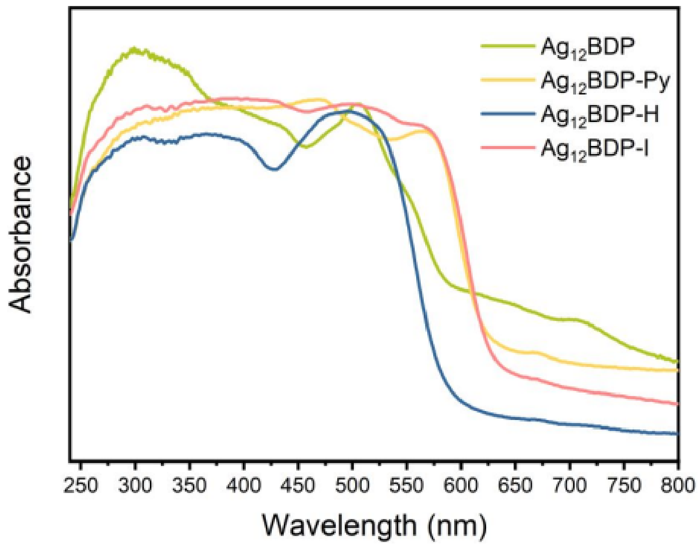

Figure S8. Solid state diffuse reflectance spectra of Ag$_{12}$-BDP, Ag$_{12}$-BDP-Py, Ag$_{12}$-BDP-H and Ag$_{12}$-BDP-I.

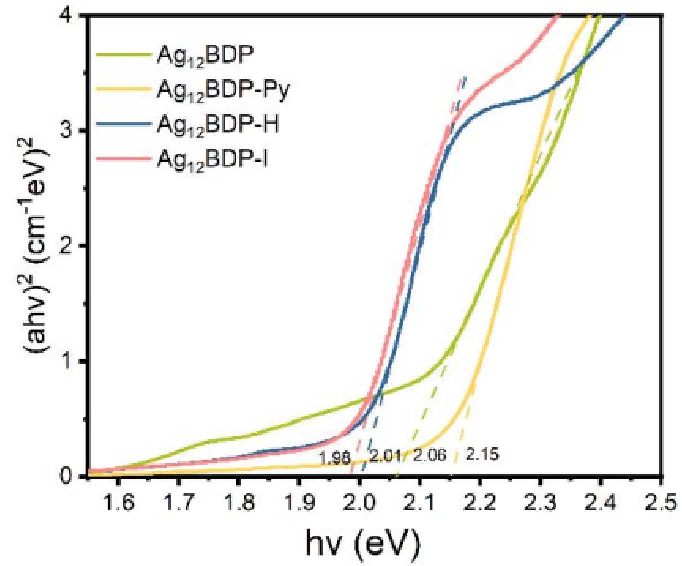

Figure S9. Tauc plots form UV-vis absorption spectra of Ag$_{12}$-BDP, Ag$_{12}$-BDP-Py, Ag$_{12}$-BDP-H and Ag$_{12}$-BDP-I.

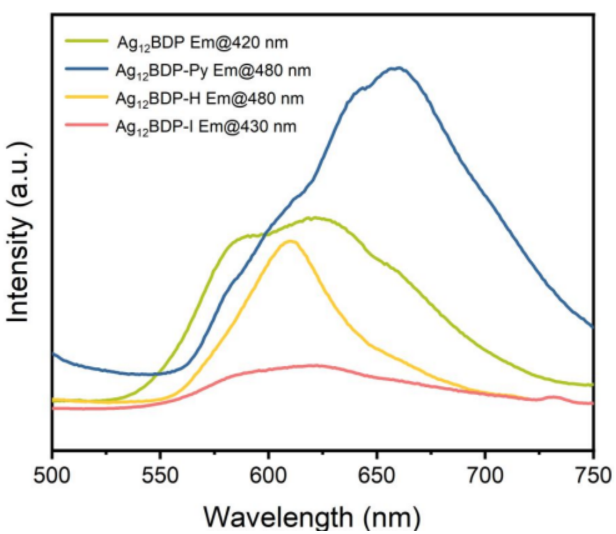

Figure S10. Emission spectra in the solid at room temperature.

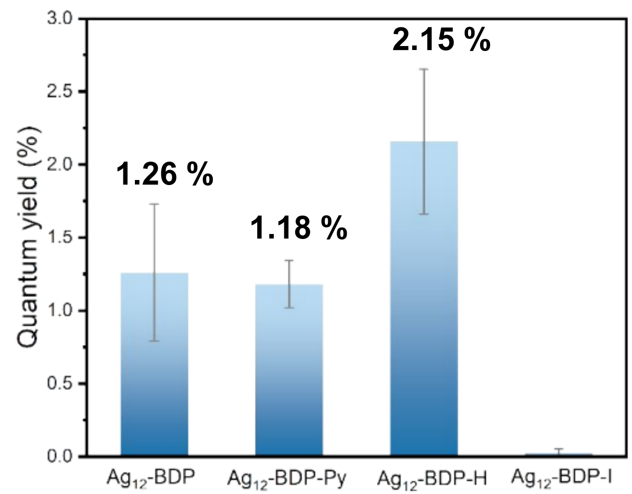

Figure S11. Quantum yield in the solid at room temperature.

	Lifetime (ns)
Ag$_{12}$-BDP	**3.0**
Ag$_{12}$-BDP-Py	**3.1**
Ag$_{12}$-BDP-H	**2.2**
Ag$_{12}$-BDP-I	**0.1**

Results and discussion

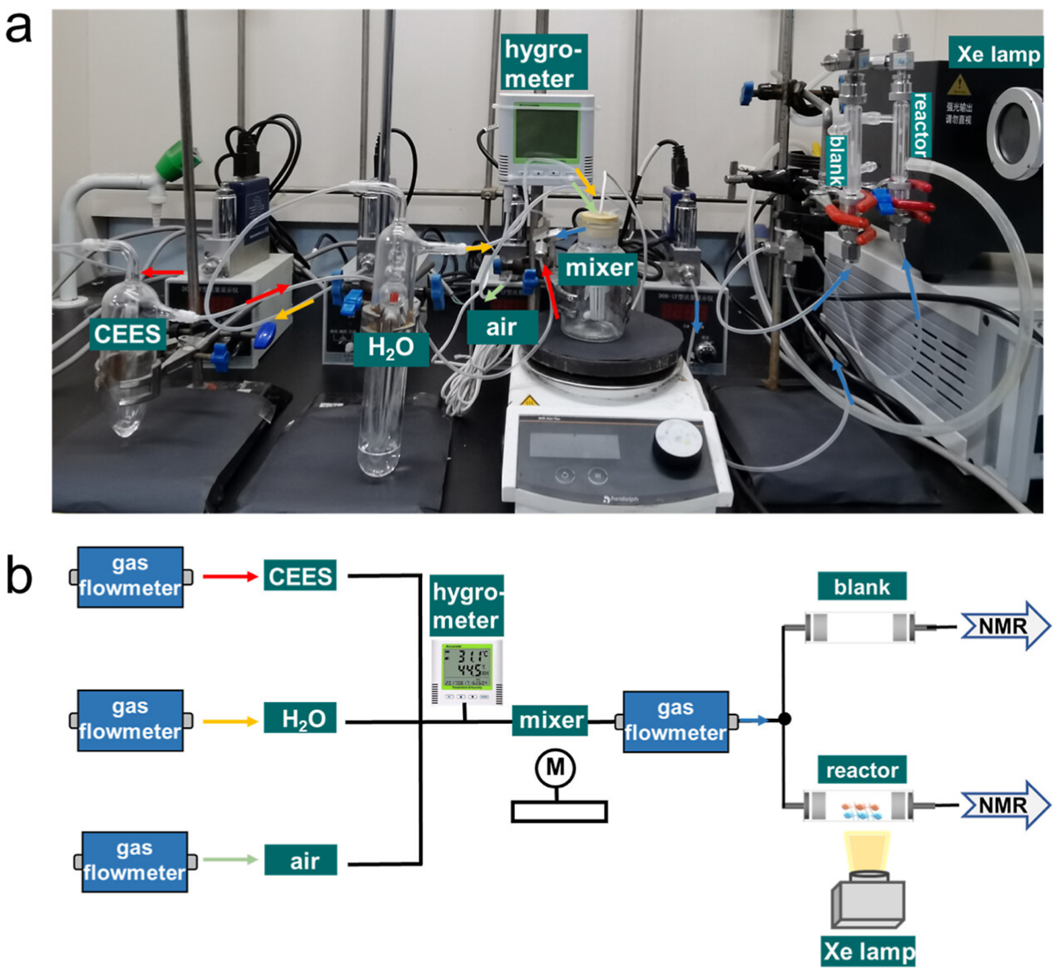

Figure 3. (a) Photograph of the continuous flow apparatus for the photooxidation of gaseous CEES under visible light irradiation. (b) Schematic illustration of the flowchart of the setup.

Sample preparation:

- **Vacuum dried at 60 °C for 6 h**
- **Ground and dispersed with quartz sand in a glass reactor**
- **Loaded into the fixed-bed continuous set-up**

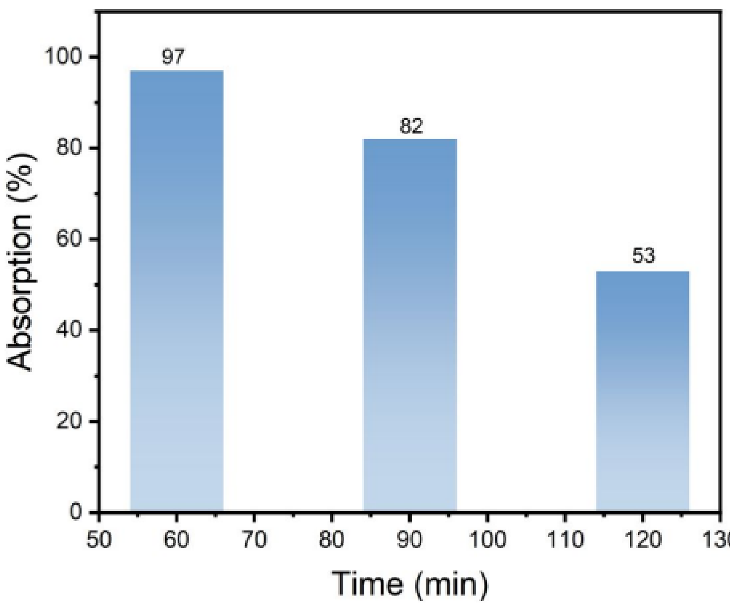

Figure S13. Adsorption capacity of Ag_{12}-BDP-I within 60, 90, and 120 min..

Results and discussion

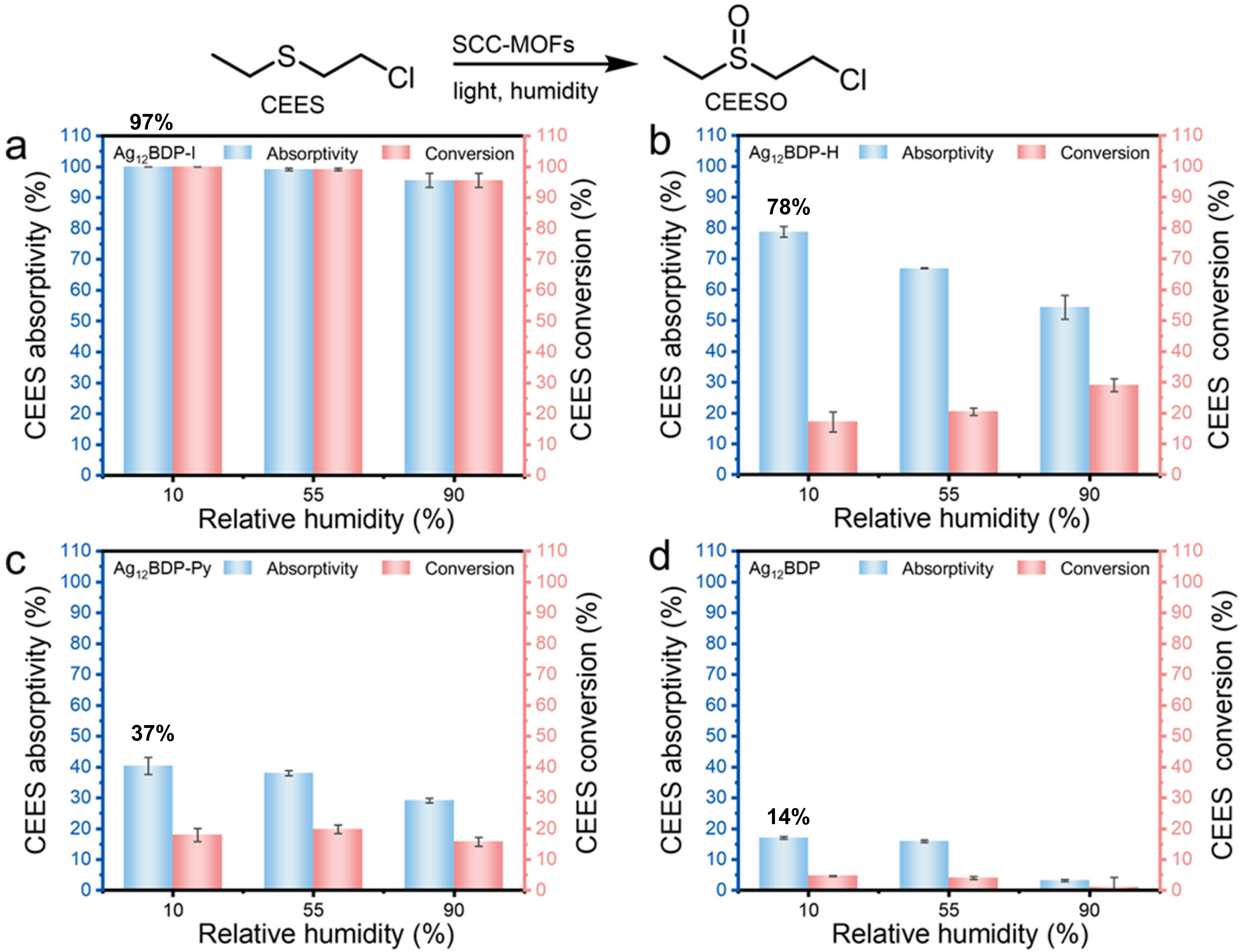

Figure 4. Absorptivity and conversion of gaseous CEES in the presence of (a) **Ag12–BDP-I**, (b) **Ag12–BDP-H**, (c) **Ag12–BDP-Py**, and (d) **Ag12–BDP** in a continuous flow apparatus under different RHs.

Results and discussion

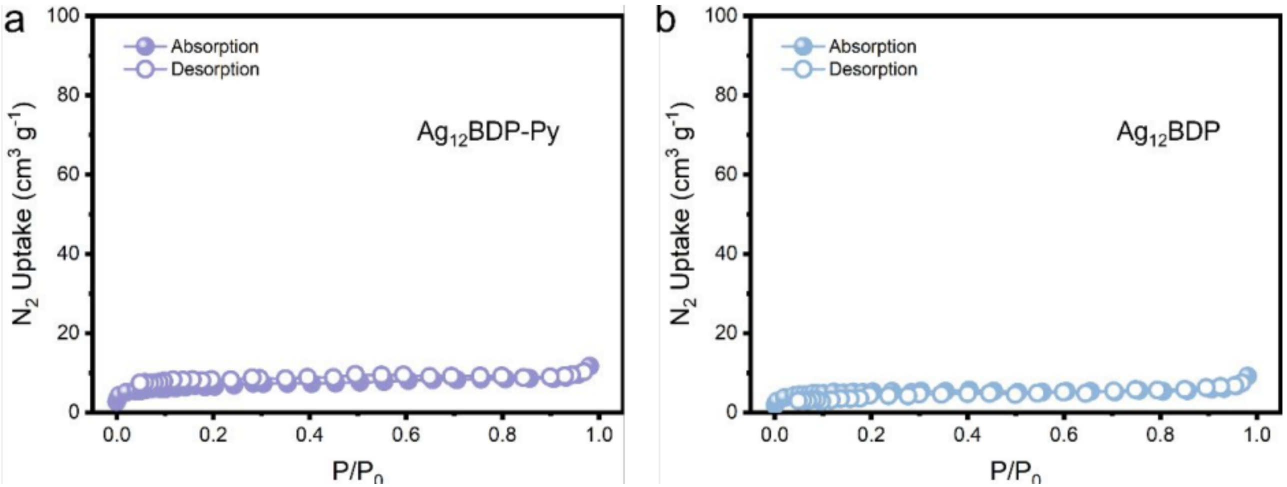

Figure S19. N_2 sorption isotherms collected at 77 K for (a) Ag_{12}-BDP-Py and (b) Ag_{12}-BDP.

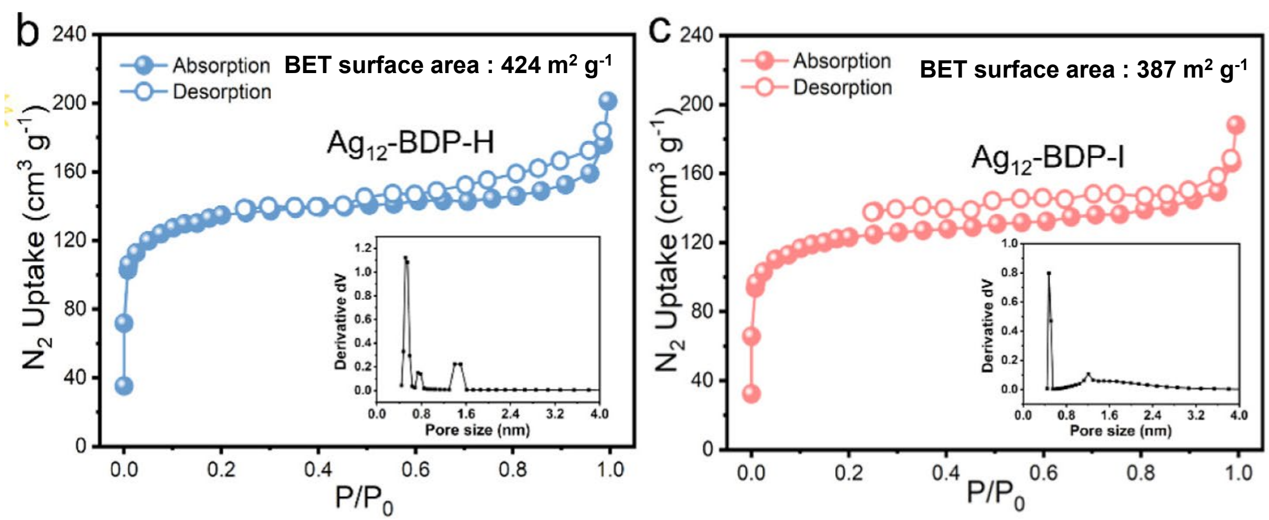

Figure 5. (b) **Ag_{12}–BDP-H** and (c) **Ag_{12}–BDP-I**. (The inset shows pore-size distributions derived from NLDFT)

Results and discussion

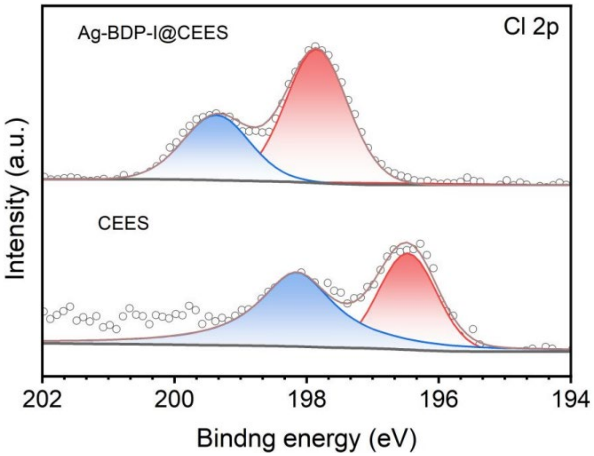

Figure S21. Cl 2p higher solution XPS spectra of CEES and Ag12-BDP-I@CEES. .

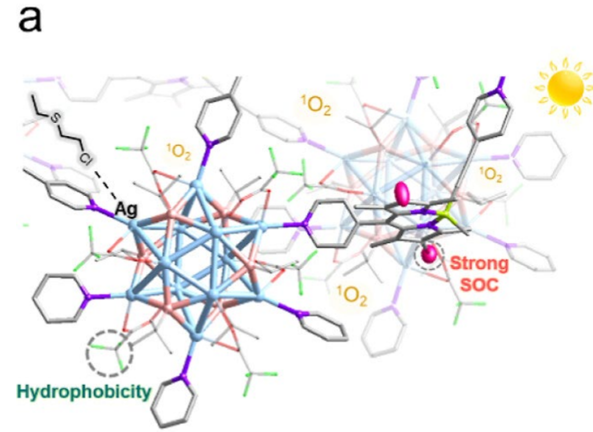

Figure 5. (a) Representative microenvironment of **Ag12–BDP-I** for gaseous CEES degradation.

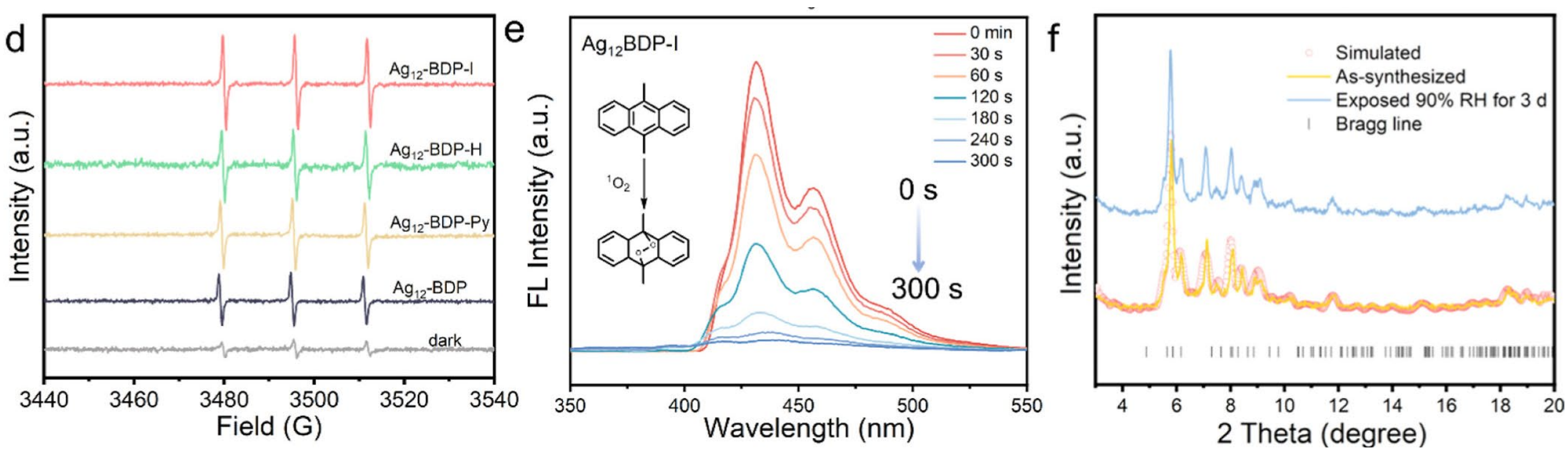

Figure 5. (d) EPR spectra of **Ag_{12}–BDP**, **Ag_{12}–BDP-Py**, **Ag_{12}–BDP-H**, and **Ag_{12}–BDP-I** mixed with 4-oxo-TMP under visible light irradiation or dark conditions. (e) Fluorescence spectra of DMA in the presence of **Ag_{12}–BDP-I** upon visible light irradiation. (f) PXRD patterns of simulated **Ag_{12}–BDP-I**, as-synthesized **Ag_{12}–BDP-I**, and **Ag_{12}–BDP-I** after exposure under 90% RH for 3 days.

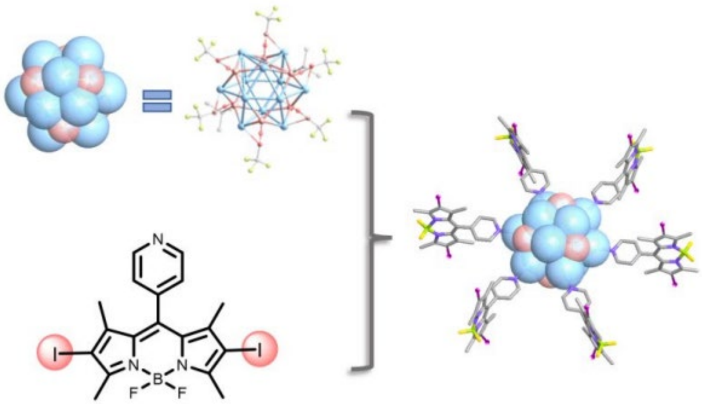

Figure S24. Overall structure of the Ag_{12}-mono-BDP-I cluster.

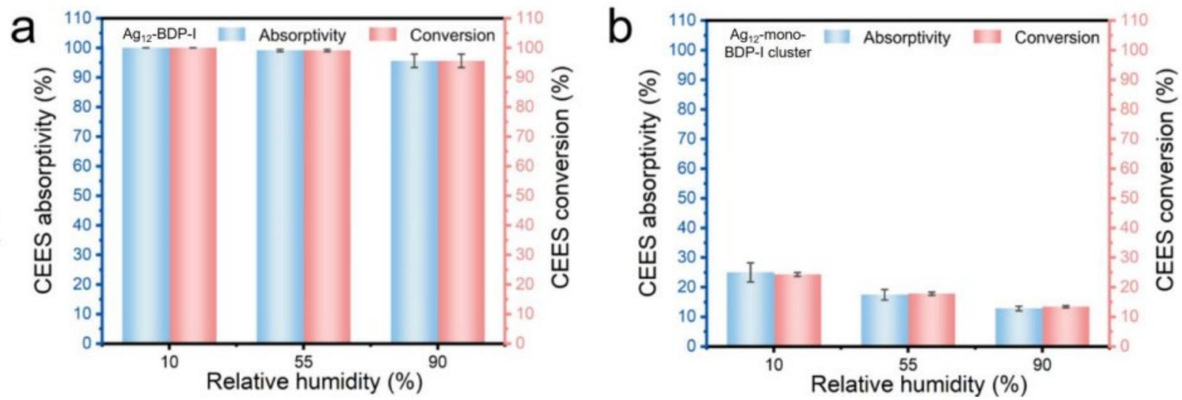

Figure S25. Absorptivity and conversion of gaseous CEES in the presence of the (a) Ag_{12}-BDP-I and the (b) Ag_{12}-mono-BDP-I cluster

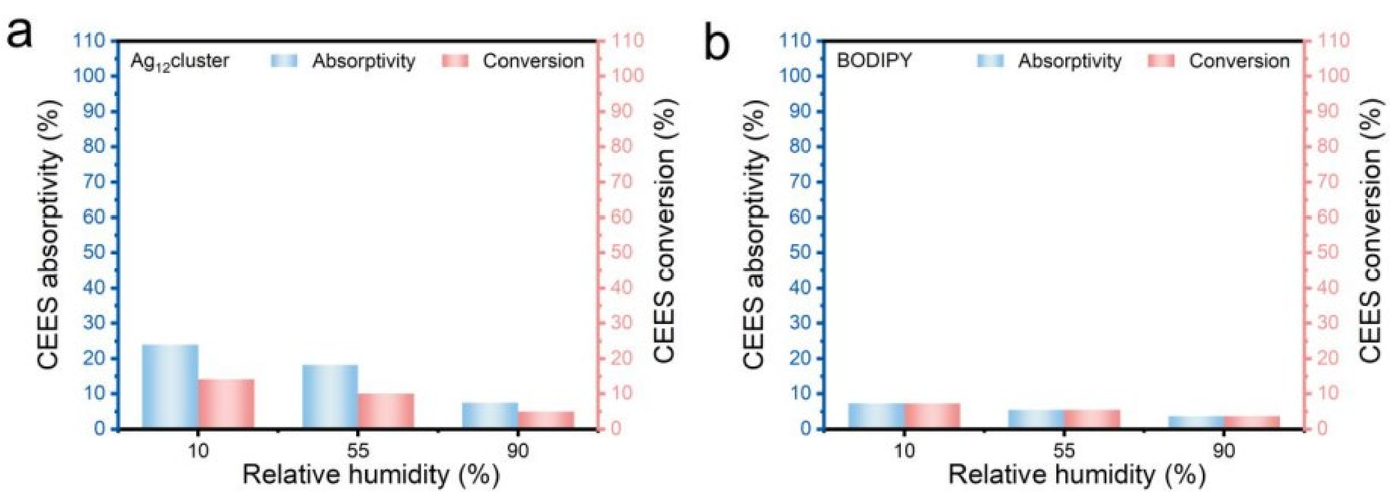

Figure S26. Absorptivity and conversion of gaseous CEES in the presence of (a) Ag_{12} clusters and (b) BODIPY.

Results and discussion

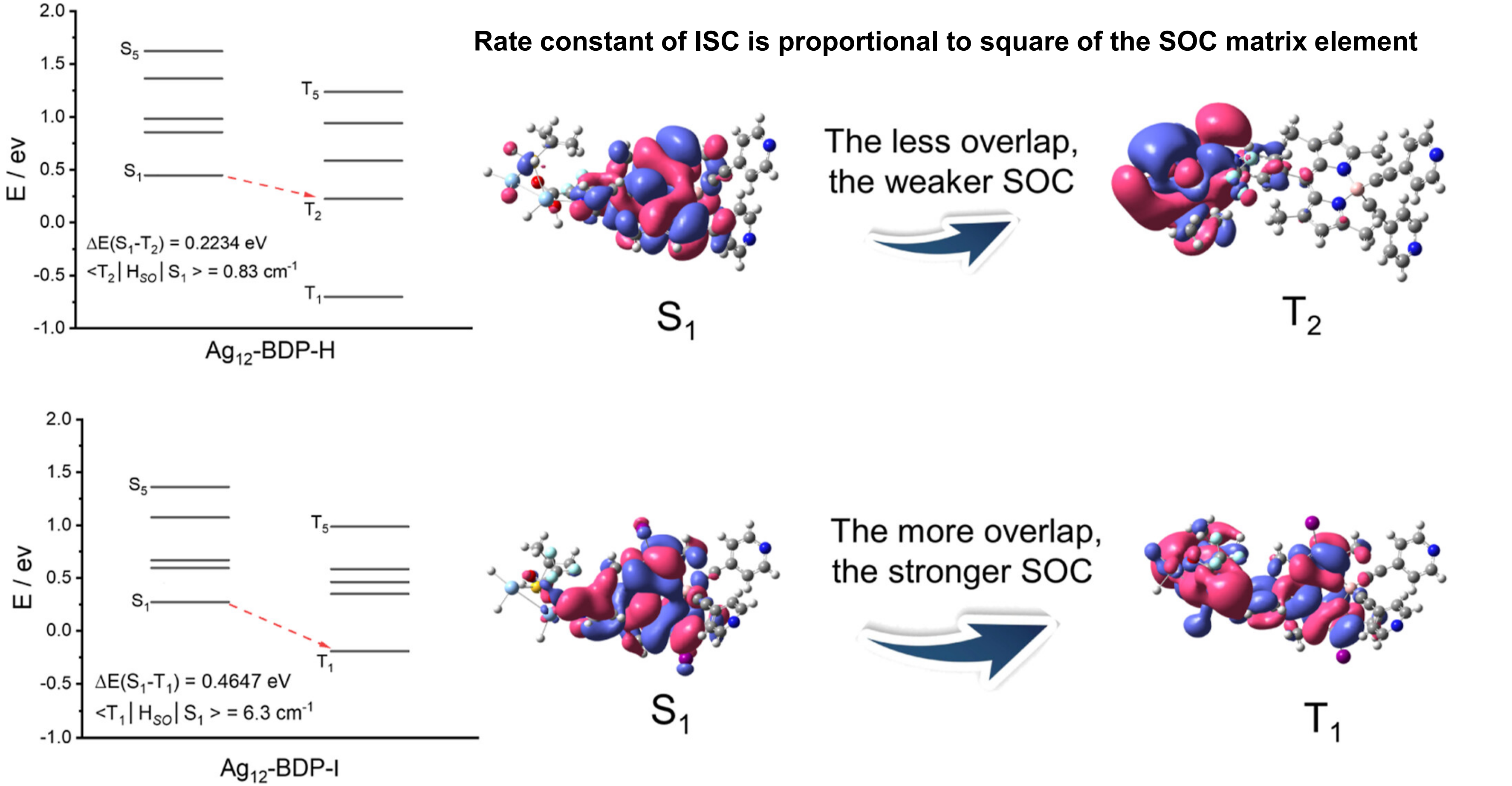

Figure 6. Energy level and orbital distribution-associated singlet and triplet states of **Ag_{12}–BDP-H** and **Ag_{12}–BDP-I**. The isovalue of the molecular orbital plot was set to 0.01.

Conclusion

- They modified the classical Ag_{12} cluster with four different functionalized BODIPY ligands to obtain a series of SCC-MOFs, namely Ag_{12}–BDP and Ag_{12}–BDP-Py, Ag_{12}–BDP-H and Ag_{12}–BDP-I.
- They examined their ability to degrade gaseous CEES by tuning its porosity, adsorption capacity and singlet oxygen generation efficiency.
- Among all of them, Ag_{12}-BDP-I shows highest efficiency in adsorption and degradation of gaseous CEES under a wide range of relative humidity from 10% to 90% due to good porosity, superior $^{1}O_2$ generation efficiency.

Thank you